Journal Pre-proofs

Increased Q-Factor Increases Medial Compartment Knee Joint Contact Force During Cycling

Tanner Thorsen, Erik Hummer, Jeffery Reinbolt, Joshua T. Weinhandl, Songning Zhang

PII: S0021-9290(21)00051-8
DOI: https://doi.org/10.1016/j.jbiomech.2021.110271
Reference: BM 110271

To appear in: *Journal of Biomechanics*

Received Date: 24 April 2020
Revised Date: 9 January 2021
Accepted Date: 16 January 2021

Please cite this article as: T. Thorsen, E. Hummer, J. Reinbolt, J.T. Weinhandl, S. Zhang, Increased Q-Factor Increases Medial Compartment Knee Joint Contact Force During Cycling, *Journal of Biomechanics* (2021), doi: https://doi.org/10.1016/j.jbiomech.2021.110271

Increased Q-Factor Increases Medial Compartment Knee Joint Contact Force During Cycling

Tanner Thorsen, Erik Hummer, Jeffery Reinbolt, Joshua T. Weinhandl, and Songning Zhang

Department of Kinesiology, Recreation and Sport Studies

The University of Tennessee, Knoxville, TN

USA

Running title: Medial Compartment Contact Force During Cycling

Corresponding Author:

Songning Zhang, PhD and FACSM
1914 Andy Holt Ave.
Knoxville, TN 37996
(P) 865-974-4716
(F) 865-974-8981
Email: szhang@utk.edu

Word Count: 3999

Abstract

As Q-Factor (QF: inter-pedal distance) is increased, the internal knee abduction moment (KAbM) also increases, however it is unknown if this increased KAbM is associated with increased medial compartment knee joint contact force in cycling. In the absence of *in vivo* measurement, musculoskeletal modeling simulations may provide a viable option for estimating knee joint contact forces in cycling. The primary purpose of this study was to investigate the effect of increasing QF on knee joint total (TCF), and medial (MCF) compartment contact force during ergometer cycling. The secondary purpose was to evaluate whether KAbM and knee extension moment are accurate predictors of MCF in cycling. Musculoskeletal simulations were performed to estimate TCF and MCF for sixteen participants cycling at an original QF (150mm), and wide QF (276mm), at 80 watts and 80 rotations per minute. Paired samples t-tests were used to detect differences between QF conditions. MCF increased significantly, however, TCF did not change at wide QF. Peak knee extensor muscle force did not change at wide QF. Peak knee flexor muscle force was significantly reduced with wide QF. Regression analyses showed KAbM and knee extension moments explained 87.4% of the variance in MCF when considered alongside QF. The increase of MCF may be attributed to increased frontal-plane pedal reaction force moment arm. Future research may seek to implement QF modulation as a part of rehabilitation or training procedures utilizing cycling in cases where medial compartment joint loading is of importance.

Keywords: Cycling, Knee Contact Force, Musculoskeletal Modeling, Q-Factor

1. Introduction

Investigation of the internal knee abduction moment (KAbM) has garnered attention in gait and cycling studies of knee osteoarthritis and total knee arthroplasty (Gardner et al., 2015; Mundermann et al., 2004; Orishimo et al., 2012). This internal joint moment indicates the muscular and ligamentous involvement around the knee joint to counteract the external knee adduction moment, commonly reported as KAM (Walter et al., 2010). It has been suggested that KAbM is associated with medial compartment contact force (MCF) at the knee, which may lead to degenerated cartilage and knee osteoarthritis (Andriacchi et al., 2009). In an effort to reduce knee medial compartment joint contact force, many studies have examined KAbM as it pertains to frontal-plane knee joint alignment (Bennett et al., 2018), gait modification (Bennett et al., 2017; Paquette et al., 2015; Shull et al., 2013), stair and ramp negotiation (Wen et al., 2019; Yocum et al., 2018), and cycling (Gardner et al., 2016; Shen et al., 2018).

Cycling is a convenient, cost effective and year-round exercise and rehabilitative modality that incorporates both aerobic and resistance training while reducing knee joint loading by placing the majority of the rider's weight on the saddle (Burke, 1986). It is during the power-phase (from 0 to 180 degrees of the crank-cycle) that the rider pushes down on the pedals and transfers the greatest amount of energy to the bicycle or ergometer (Asplund and St Pierre, 2004). Thus, peak pedal reaction force (PRF), knee extension moment (KEM), KAbM, and total knee joint contact force (TCF) have been shown to occur during the power-phase of the crank-cycle (Kutzner et al., 2012).

Q-Factor (QF) refers to the horizontal distance between bike pedals (Disley and Li, 2014). Recently, we have found that increasing QF during ergometer cycling increases peak KAbM without changing peak KEM during the power-phase (Thorsen et al., 2020). The relationship

between increased KAbM, as a result of increased QF, and knee joint contact forces remains unknown. If increased QF produces increased KAbM but not KEM, it is plausible then that MCF may increase while TCF would remain unchanged. This would suggest that QF could modulate MCF without changing overall knee joint loading, as represented by TCF.

Although the inverse dynamics-based calculation of KAbM is often used as a surrogate to knee medial compartment joint loading, it is not a direct measurement of MCF. Moreover, it has been shown that KAbM does not correspond to MCF well in certain walking tasks (Manal et al., 2015; Walter et al., 2010). Walter et al. (2010) suggested that KAbM be considered in conjunction with KEM during walking tasks due to the possibility of increased joint compression. In cycling, it is not known if KAbM is an accurate predictor of MCF. Understanding the relationship between KAbM and MCF in cycling may provide retrospective support for cycling studies which have examined ways to decrease MCF as represented by KAbM (Gardner et al., 2015; Thorsen et al., 2020), as well as prospective rationale for future cycling intervention research of similar purpose.

Joint contact force is primarily a product of forces produced by muscles acting on the joint (Sasaki and Neptune, 2010). In the absence of *in vivo* measurements using an instrumented knee prosthesis, musculoskeletal modeling and simulations may provide a viable option for estimation of knee joint contact forces by producing necessary information, such as individual muscle forces, that allow for an accurate estimation of TCF (Walter et al., 2010). Recent musculoskeletal models have improved the estimation of TCF, even allowing for the resolution of MCF and lateral knee compartment contact force (Lerner et al., 2015).

The purpose of this study was to investigate the effect of increasing QF on TCF and MCF during ergometer cycling and evaluate whether KAbM and KEM are accurate predictors of MCF

in cycling. We hypothesized that MCF would increase while TCF would remain unchanged with increased QF, and that a significant proportion of the variance in MCF would be explained by KAbM, and that the explained variance of MCF would further increase with addition of KEM and QF.

2. Method

2.1 Participants

Sixteen recreationally active young adults (8 male, 8 female age: 22.4 ± 2.6 yr, height: 1.74 ± 0.11 m, mass: 69.20 ± 9.75 kg, BMI: 22.78 ± 1.43 kg/m^2) participated in this study. Participants were excluded from the study if they had a major lower extremity musculoskeletal injury within the past 6 months or had a body mass index > 25 kg/m^2. All participants provided written informed consent approved by the university institution review board.

2.2 Experimental Procedures

Full details of kinematic and kinetic data collection have been previously described (Thorsen et al., 2020). Participants cycled on a cycle ergometer at 4 different QFs and 3 different workrates while 3D kinematic (240Hz, Vicon Motion Analysis Inc., Oxford, UK) and PRF data using two customized instrumented pedals (1200 Hz, Type 9027C, Winterthur, Kistler, Switzerland) were collected for 5 consecutive pedal cycles. For this current analysis, two QF conditions were considered while cycling at a workrate of 80 watts and 80 rotations per minute (RPM); QF of 150 mm (normal QF), which is the manufactured QF, as well as QF of 276 mm (wide QF).

2.3 Instrumentation

An open source musculoskeletal model (18 segments, 23 degrees-of-freedom (DOF), 92 muscle-tendon actuators) capable of resolving knee MCF and TCF was used in the

musculoskeletal simulation (Lerner et al., 2015). The knee joint of this model consists of 1 DOF (flexion/extension) supplemented with added medial and lateral compartments (Lerner et al., 2015). The model was scaled to each participant's height and mass and the subtalar and metatarsal-phalangeal joints were locked. Pelvic tilt angle for all cycling trials was increased uniformly by 13 degrees to account for the offset between the clinical definition of the neutral pelvis and the model definition of the neutral pelvis (i.e. pelvic tilt = 0 degrees).

Generalized joint coordinates derived from inverse kinematics calculations were exported from Visual3D (Version 6, C-Motion, Inc., Germantown, MD, USA). These kinematics were applied to each subject-specific musculoskeletal model. Inverse dynamics calculations were performed in OpenSim to compute lower extremity joint moments (v3.3 OpenSim, SimTK, Stanford University). Next, muscle activations and forces during cycling were calculated using static optimization (Steele et al., 2012). The static optimization calculations included muscle physiology (force-length-velocity relationships) and an objective function to minimize the sum of squared muscle activations (Crowninshield and Brand, 1981). Maximum reserve torque actuator values for all lower extremity joints were checked and found to be within suggested guidelines (Hicks et al., 2015). Joint contact forces (TCF, MCF) were calculated using joint reaction analysis in OpenSim and expressed in the tibia reference frame (Steele et al., 2012).

The frontal-plane moment arm was calculated as the perpendicular distance from the knee joint center to the frontal-plane resultant PRF, which was transformed into the shank reference frame. The frontal-plane moment arm was calculated as the quotient of KAbM and the frontal-plane PRF. Moment arms at the time of peak KAbM was identified for subsequent analysis.

2.4 Data and statistical analysis

Variables of interest included peak power-phase KEM, KAbM, TCF, MCF, frontal-plane moment arm at the time of peak KAbM as well as peak forces of the knee extensor [rectus femoris (RF), vastus lateralis (VL), vastus intermedius, and vastus medialis (VM)] and knee flexor (biceps femoris long and short heads (BF), semimembranosus, semitendinosus (ST), sartorius, gracilis, and both medial and lateral head of the gastrocnemius) muscle groups. Peak kinetic variables and muscle forces for the power-phase of each crank-cycle were identified using a custom MATLAB program (2019a, MathWorks, Inc., Natick, MA).

Paired samples t-tests were performed in MATLAB to compare peak joint moments, contact forces, frontal-plane moment arms and muscle forces during the power-phase between normal and wide QF conditions. The *a priori* significance level was set at $p < .05$ with effect sizes calculated using Cohen's d (Cohen, 2013). Analysis of individual subject peak MCF values indicated that a small subset of participants (n = 4, 'non-responder') exhibited decreased peak MCF with wide QF. The remining subset of participants (n = 12, 'responder') all exhibited increased peak MCF with wide QF. Additional paired samples t-tests were performed with the responders' data set. Due to the small sample size of the non-responder subset group, simple effect sizes were calculated; however, we elected to not perform additional statistical analysis.

The ability of KAbM to predict corresponding MCF was first examined with a linear regression analysis in which KAbM and KEM were input as predictor variables and MCF at normal QF as the outcome variable (25.0 IBM SPSS, Chicago, IL). A multivariate linear regression model was also performed to assess whether a combination of KAbM and KEM predicted MCF at normal QF better than those variables individually. Multivariate linear regression models were also performed to assess whether a combination of peak KAbM and KEM, and QF (both normal and wide QF) predicts peak MCF better than KAbM alone for

cycling.

3. Results

For the entire group, wide QF had larger peak power-phase MCF ($p = 0.025$, d = 0.51 Table 1 and Figure 1). There were no differences in the magnitudes of peak power-phase TCF between normal and wide QFs. The knee flexor group produced lower peak power-phase muscle force at wide QF (p = 0.046, d = 0.45, Table 2). There was no difference in the force production of the knee extensors muscle group between QF conditions. Peak RF and biceps femoris muscle forces increased with wide QF, while peak ST muscle force decreased (Table 2). The frontal-plane moment arm at the time of peak KAbM was significantly greater at wide QF (Table 1).

Muscle activation patterns for normal and wide QF for select knee-spanning muscles determined from static optimization are presented in Figure 3. Qualitatively, RF had greater activation during wide QF compared to normal QF. Inverse dynamics calculations of KAbM and KEM using this single DOF knee joint indicate that KAbM increased ($p < 0.001$, d = 0.87) and KEM remained unchanged with wide QF for the entire group (Table 1, Figure 4).

For the responder subset group, increases of KAbM (p = 0.001, d = 0.95) and MCF (p = 0.001, d = 0.91) were observed at wide QF (Table 1, Figure 5). There were no changes of KEM, TCF, or muscle forces for the responder subset group at wide QF. At wide QF, the non-responder subset group mean MCF decreased by nearly 96 N, while mean TCF decreased by 129 N. Mean KAbM increased by 3.0 Nm while mean KEM decreased by 0.9 Nm.

Linear regression analysis with normal QF data indicated that the inclusion of both KAbM and KEM improved the prediction of MCF and resulted in the highest R^2 of 81% (explained variance) with the second lowest root mean square error (RMSE), compared to separate regression models using either KAbM or KEM alone as a predictor variable (Table 3).

Predicting MCF from a combination of KAbM, KEM, and QF improved the prediction of MCF, yielding an R^2 value explaining 87% of the variation in MCF with the second lowest RMSE (Table 4). Although peak KAbM did not result in the highest R^2 value, it yielded the lowest RMSE value when included as the single independent variable in both models (Table 3 and 4).

4. Discussion

This study aimed to investigate the effect of increasing QF on TCF and MCF during ergometer cycling. A secondary purpose was to evaluate whether KAbM and KEM are accurate predictors of corresponding changes in MCF in cycling. It was hypothesized that MCF would increase while TCF would remain unchanged with increased QF.

Our primary hypothesis was supported as MCF for the entire group increased by 12% and TCF did not change. We have previously shown that increased QF increases peak KAbM (Thorsen et al., 2020). In this study, similar changes were observed as both MCF and KAbM increased with wide QF. It is important to observe that overall joint loading, as indicated by TCF and KEM, remained unchanged. Thus, increasing the QF from normal to wide only significantly increased the knee medial compartment joint loading without affecting the knee overall loading patterns. Although it may sound counter-intuitive, future research may seek to implement QF modulation as part of rehabilitation or training procedures utilizing cycling in cases where consideration of medial compartment joint contact force is of importance. Modulating medial compartment knee contact force in a graded manner during stationary cycling, through increases of QF, may promote healthy adaptation to tolerable joint contact force and improve muscle weakness.

The waveforms of MCF and TCF presented in Figure 1 are bimodal, with peaks at similar timing as the muscle forces during the power-phase (~90° of the crank-cycle), as well as at the

recovery-phase (~180° of the crank-cycle). This observation aligns with previously reported instrumented knee prostheses data obtained during cycling (Kutzner et al., 2012). Although Kutzner et al. (2012) did not report MCF, analysis of the data used in the study (accessed at www.orthoload.com) indicates that peak power-phase TCF while cycling at 75 watts and 60 RPM (the most similar condition to present study) was 907 N, occurring in the first 90° in the crank-cycle. Peak power-phase TCF in this study is of similar magnitude at 882.9 N, notwithstanding a much younger population cycling at 80 watts and 80 RPM.

In the context of joint contact force, it is important to consider the forces produced by muscles acting on the joint. In this study we examined peak power-phase muscle forces for the knee extensors and knee flexors (Table 2, Figure 1C,D). Although the global peak knee extensor muscle forces did not change with increased QF, they did occur at the same time as the peak power-phase MCF and TCF (Figure 1A,B). The consistent power-phase peak muscle forces between the two QFs may support consistent power-phase TCF and KEM with increased QF but does not explain increased MCF and KAbM. Increased KAbM is the product of an increased moment arm of the frontal-plane PRF vector to the knee joint center. This increased moment arm increases the external knee adduction torque, thereby increasing KAbM (Thorsen et al., 2020). Frontal-plane moment arm at the time of peak KAbM increased by 36% from normal to wide QF. Moment arm is largely dictated by the location of the knee joint center and the magnitude of the mediolateral pedal reaction force. Thus, the magnitude of KAbM is heavily influenced by the mediolateral PRF as it increases throughout the crank cycle, overwhelming the influence of the moment arm. This increased external knee adduction moment may also increase compression on the medial compartment of the knee, thereby increasing MCF. Since the muscles used in the musculoskeletal model actuate only the sagittal plane DOF of the knee, MCF may be increased

from the dynamic coupling of non-knee-spanning muscles (i.e. hip-spanning muscles acting on the femur) (Neptune et al., 2000). The global peak knee flexor forces occurred at the same time as the peak recovery-phase MCF and TCF. This strategy of a knee extensor driven power-phase with a knee flexor driven recovery-phase has been previously proposed as the muscular control strategy by which the knee joint is actuated during cycling (Neptune et al., 2000; Raasch and Zajac, 1999). Although the knee flexors demonstrated a significantly different peak power-phase muscle force, at around 45° of the crank-cycle, these peaks did not temporally align with the peak values of MCF and likely did not contribute to the increased peak MCF near 90° of the crank-cycle. Additionally, VM force seems to play a minor role in contribution to MCF (Supplementary material 1).

Muscle activation patterns from this study generally agreed with published EMG linear envelope patterns found in the cycling literature (Ryan and Gregor, 1992; Savelberg et al., 2003). Activation profiles of the biceps femoris, VL, and VM in this study indicate that peak activations occur at similar times during the crank-cycle as do those presented by Ryan et al. (1992). Peak activation for the medial head of the gastrocnemius and the ST occurred later in the crank-cycle than reported by Ryan et al. (1992), however, agree with muscle activations presented by Savelberg et al. (2003) (Figure 3A). Peak activation for the RF muscle is observed at about 90° of the crank-cycle (Figure 3C), however Ryan et al. (1992) reported decreasing activation (Figure 3C) while Savelberg et al. (2003). (1998) reported peak activation of the RF at similar times in the crank-cycle (Figure 3C). Although Savelberg normalized their EMG signals to values obtained from one of their test conditions, making the magnitudes of activations not comparable, their reported timings of the activations of ST and RF muscles are agreeable with our simulated muscle activations. RF had a greater muscle activation at wide QF compared with

normal QF, which provides support for the increase of muscle force generated by RF (Table 2). Differences in activation patterns in this current study may be attributable to the time-independent characteristics of static optimization (Anderson and Pandy, 2001; Hardt, 1978) as well as differences in pedal/shoe interface (i.e. cleated shoes, clipless pedals, and toe-cages). Future work may seek to identify changes in lower extremity EMG patterns as a result of different shoe/pedal interfaces.

Our regression models offer robust prediction of MCF from KAbM and KEM. In our study, peak values of MCF, KAbM, and KEM were obtained for five consecutive crank-cycles and averaged for each participant, resulting in data points from 16 participants. The number of data points was doubled with the inclusion of wide QF in the second set of regression models. The second set of regression analyses also showed that peak power-phase MCFs during cycling were best predicted by a combination of KAbM, KEM and QF. In both sets of models, KAbM was better able to predict peak power-phase MCF when included alongside KEM, than the regression models using either KAbM or KEM alone (Table 3 & 4). This finding agrees with Walter et al. (2010) who suggested that KEM tends to increase overall joint compression, and therefore affects MCF. Walter et al. (2010) predicted peak values of MCF via peak KAbM, and KEM from 15 trials of three different walking conditions (normal walking, medial-thrust gait, and walking poles) from one single participant in their regression models. They reported R^2 values ranging from 0.57 using only KAbM, to 0.93 using KAbM and KEM for both loading-response and push-off peak MCFs. Incorporating KAbM, KEM, and QF as predictor variables in this study produced the best predictive capabilities with over 87% explained variance of MCF. These findings, in conjunction with peak knee flexor and extensor muscle forces, suggest that increases of MCF during cycling may be more complex than indicated by changes to KAbM alone.

Prediction of MCF in cycling from KAbM and KEM is also similar to prediction of MCF in gait. Future research may consider induced acceleration analysis, providing additional insight on how hip and ankle muscles influence MCF.

Increased MCF was not demonstrated by all participants, as a small subset of the sample demonstrated decreased MCF with wide QF. Qualitative analysis of MCF between the two subset groups revealed that the magnitude of increase MCF for the responder group was 24% with increased QF (-627.7 N vs. -777.1 N), as compared to the overall sample increase of 12% (-639.1 N vs. -717.2 N). The non-responder group decreased MCF by 12% (-673.2 N vs. -577.5 N). Several researchers have identified subsets of samples which have had adverse biomechanical responses to gait modifications aimed at manipulating KAbM in persons with knee OA (Erhart-Hledik et al., 2017; Hinman et al., 2012). In the case of this study, it is possible that subject-specific characteristics such as frontal-plane lower limb alignment, strength, and age may have confounded the effect of the modification (i.e. increased QF) on joint contact force.

Several limitations need to be acknowledged from this work. The musculoskeletal model used in this study has been validated against contact forces obtained from an instrumented knee prosthesis for level walking (Lerner et al., 2015), but has yet to be validated for cycling. Future work should validate this model with *in vivo* cycling data. Additionally, subject-specific medial and lateral condyle contact points were not implemented in this study, which could hamper contact force estimation accuracy (Lerner et al., 2015).

There has been criticism of musculoskeletal models that make simplifying assumptions, such as a single DOF knee joint (Marouane et al., 2017). Utilizing methods such as finite element with musculoskeletal modeling, researchers have shown that more complex models may accurately predict non-sagittal plane joint moments. Given the validation of the knee model used in this

current study against in-vivo instrumented knee contact force data (Lerner et al., 2015), we feel this model provides accurate estimation of knee joint contact forces and is a suitable tool for testing our hypotheses. It has also been suggested that the knee adduction angle, as opposed to KAbM, may be a more primary parameter to consider in regard to medial compartment knee joint loading (Marouane and Shirazi-Adl, 2019). Given the simplifying single DOF assumption of the musculoskeletal model used in this study, analysis of frontal-plane knee angles is not possible. Our previous work, however, did utilize a hybrid six DOF knee joint (Thorsen et al., 2020), and showed that increasing from normal to wide QF did not significantly change the peak knee adduction angles.

Although the activations of the RF and ST muscles are different from that of Ryan et al. (1992), the RF and ST activations are more similar to those found by Savelberg et al. (2003), and RF activation is also similar to that of the two vasti muscles activations in this study. Additionally, Figure 1D shows that the timing of peak muscle force of the knee flexor muscle group is not aligned with the timing of peak contact forces. Therefore, the contribution from the ST muscle to peak knee joint contact forces is likely very low. Given the objective function of our static optimization criteria, the net joint moments must be matched when determining muscle activations and forces. If a different optimization method was used, a different set of muscle activations may be found. Furthermore, there are an infinite number of combinations of muscles forces that could produce the same net joint moment, yet theoretically produce different joint contact forces. If the RF muscle, for example, was activated to a greater magnitude, it would produce more muscle force. In order for the net joint moment to remain constant, muscle forces from the three vasti muscles would need to be reduced likely through different activation patterns. VM and VL have greater cross-sectional areas and maximum isometric muscles forces

and produce greater muscle forces throughout the crank cycle than RF. Furthermore, since all quadricep muscles share a common insertion on the tibial tuberosity via the patellar tendon, differing distributions of muscle forces amongst the four knee extensors are not likely to generate dramatically different knee frontal-plane joint moments or contact forces. With the good agreement between our predicted total contact force and in vivo total contact force obtained by Kutzner et al. (2012), in addition to our joint moments being consistent with literature, our results present reasonable and physiological contact forces.

In summary, increasing QF during cycling increases MCF but does not affect TCF. There was no difference in peak power-phase knee extensor muscle force, however increased QF resulted in decreased peak power-phase knee flexor muscle force. A combination of KAbM, KEM, and QF predicted peak MCF with the best accuracy, explaining 87% of the variance. Without the inclusion of QF as an independent variable, the best accuracy in peak MCF prediction was achieved through a combination of peak KAbM and KEM. Future research may seek to implement QF modulation as part of rehabilitation or training procedures utilizing cycling in cases where medial compartment joint contact force is of importance. Modulating knee medial compartment contact force in a graded manner during stationary cycling, through increases of QF, may promote healthy adaptation to tolerable joint loading and improve muscle weakness.

References

Anderson, F.C., Pandy, M.G., 2001. Static and dynamic optimization solutions for gait are practically equivalent. J Biomech 34, 153-161

Andriacchi, T.P., Koo, S., Scanlan, S.F., 2009. Gait mechanics influence healthy cartilage morphology and osteoarthritis of the knee. The Journal of bone and joint surgery. American volume 91 Suppl 1, 95-101.10.2106/JBJS.H.01408

Asplund, C., St Pierre, P., 2004. Knee pain and bicycling: fitting concepts for clinicians. The Physician and sportsmedicine 32, 23-30.10.3810/psm.2004.04.201

Bennett, H.J., Shen, G., Cates, H.E., Zhang, S., 2017. Effects of toe-in and toe-in with wider step width on level walking knee biomechanics in varus, valgus, and neutral knee alignments. The Knee 24, 1326-1334.10.1016/j.knee.2017.08.058

Bennett, H.J., Weinhandl, J.T., Fleenor, K., Zhang, S., 2018. Frontal Plane Tibiofemoral Alignment is Strongly Related to Compartmental Knee Joint Contact Forces and Muscle Control Strategies during Stair Ascent. J Biomech Eng 140, 061011.10.1115/1.4039578

Burke, E., 1986. Science of cycling. Human Kinetics Publishers.

Cohen, J., 2013. Statistical power analysis for the behavioral sciences. Academic press.

Crowninshield, R.D., Brand, R.A., 1981. A physiologically based criterion of muscle force prediction in locomotion. J Biomech 14, 793-801

Disley, B.X., Li, F.X., 2014. The effect of Q factor on gross mechanical efficiency and muscular activation in cycling. Scand J Med Sci Sports 24, 117-121.10.1111/j.1600-0838.2012.01479.x

Erhart-Hledik, J.C., Asay, J.L., Clancy, C., Chu, C.R., Andriacchi, T.P., 2017. Effects of active feedback gait retraining to produce a medial weight transfer at the foot in subjects with symptomatic medial knee osteoarthritis. Journal of orthopaedic research : official publication of the Orthopaedic Research Society 35, 2251-2259.10.1002/jor.23527

Gardner, J.K., Klipple, G., Stewart, C., Asif, I., Zhang, S., 2016. Acute effects of lateral shoe wedges on joint biomechanics of patients with medial compartment knee osteoarthritis during stationary cycling. J Biomech 49, 2817-2823.10.1016/j.jbiomech.2016.06.016

Gardner, J.K., Zhang, S., Liu, H., Klipple, G., Stewart, C., Milner, C.E., Asif, I.M., 2015. Effects of toe-in angles on knee biomechanics in cycling of patients with medial knee osteoarthritis. Clin Biomech (Bristol, Avon) 30, 276-282.10.1016/j.clinbiomech.2015.01.003

Hardt, D.E., 1978. Determining muscle forces in the leg during normal human walking—an application and evaluation of optimization methods.

Hicks, J.L., Uchida, T.K., Seth, A., Rajagopal, A., Delp, S.L., 2015. Is my model good enough? Best practices for verification and validation of musculoskeletal models and simulations of movement. Journal of biomechanical engineering 137

Hinman, R.S., Bowles, K.A., Metcalf, B.B., Wrigley, T.V., Bennell, K.L., 2012. Lateral wedge insoles for medial knee osteoarthritis: effects on lower limb frontal plane biomechanics. Clin Biomech (Bristol, Avon) 27, 27-33.10.1016/j.clinbiomech.2011.07.010

Kutzner, I., Heinlein, B., Graichen, F., Rohlmann, A., Halder, A.M., Beier, A., Bergmann, G., 2012. Loading of the knee joint during ergometer cycling: telemetric in vivo data. The Journal of orthopaedic and sports physical therapy 42, 1032-1038.10.2519/jospt.2012.4001

Lerner, Z.F., DeMers, M.S., Delp, S.L., Browning, R.C., 2015. How tibiofemoral alignment and contact locations affect predictions of medial and lateral tibiofemoral contact forces. J Biomech 48, 644-650

Li, L., Caldwell, G.E., 1998. Muscle coordination in cycling: effect of surface incline and posture. J Appl Physiol (1985) 85, 927-934.10.1152/jappl.1998.85.3.927

Manal, K., Gardinier, E., Buchanan, T.S., Snyder-Mackler, L., 2015. A more informed evaluation of medial compartment loading: the combined use of the knee adduction and flexor moments. Osteoarthritis and cartilage 23, 1107-1111

Marouane, H., Shirazi-Adl, A., 2019. Sensitivity of medial-lateral load sharing to changes in adduction moments or angles in an asymptomatic knee joint model during gait. Gait & posture 70, 39-47

Marouane, H., Shirazi-Adl, A., Adouni, M., 2017. 3D active-passive response of human knee joint in gait is markedly altered when simulated as a planar 2D joint. Biomechanics and modeling in mechanobiology 16, 693-703

Mundermann, A., Dyrby, C.O., Hurwitz, D.E., Sharma, L., Andriacchi, T.P., 2004. Potential strategies to reduce medial compartment loading in patients with knee osteoarthritis of varying severity: reduced walking speed. Arthritis and rheumatism 50, 1172-1178.10.1002/art.20132

Neptune, R.R., Kautz, S., Zajac, F., 2000. Muscle contributions to specific biomechanical functions do not change in forward versus backward pedaling. J Biomech 33, 155-164

Orishimo, K.F., Kremenic, I.J., Deshmukh, A.J., Nicholas, S.J., Rodriguez, J.A., 2012. Does total knee arthroplasty change frontal plane knee biomechanics during gait? Clinical Orthopaedics and Related Research® 470, 1171-1176

Paquette, M.R., Klipple, G., Zhang, S., 2015. Greater Step Widths Reduce Internal Knee Abduction Moments in Medial Compartment Knee Osteoarthritis Patients During Stair Ascent. Journal of applied biomechanics 31, 229-236.10.1123/jab.2014-0166

Raasch, C.C., Zajac, F.E., 1999. Locomotor strategy for pedaling: muscle groups and biomechanical functions. J Neurophysiol 82, 515-525.10.1152/jn.1999.82.2.515

Ryan, M.M., Gregor, R.J., 1992. EMG profiles of lower extremity muscles during cycling at constant workload and cadence. Journal of Electromyography and Kinesiology 2, 69-80.10.1016/1050-6411(92)90018-e

Sasaki, K., Neptune, R.R., 2010. Individual muscle contributions to the axial knee joint contact force during normal walking. J Biomech 43, 2780-2784.10.1016/j.jbiomech.2010.06.011

Savelberg, H.H., Van de Port, I.G., Willems, P.J., 2003. Body configuration in cycling affects muscle recruitment and movement pattern. Journal of Applied Biomechanics 19, 310-324

Shen, G., Zhang, S., Bennett, H.J., Martin, J.C., Crouter, S.E., Fitzhugh, E.C., 2018. Effects of Knee Alignments and Toe Clip on Frontal Plane Knee Biomechanics in Cycling. J Sports Sci Med 17, 312-321

Shull, P.B., Shultz, R., Silder, A., Dragoo, J.L., Besier, T.F., Cutkosky, M.R., Delp, S.L., 2013. Toe-in gait reduces the first peak knee adduction moment in patients with medial compartment knee osteoarthritis. J Biomech 46, 122-128.10.1016/j.jbiomech.2012.10.019

Steele, K.M., DeMers, M.S., Schwartz, M.H., Delp, S.L., 2012. Compressive tibiofemoral force during crouch gait. Gait & posture 35, 556-560

Thorsen, T., Strohacker, K., Weinhandl, J.T., Zhang, S., 2020. Increased Q-Factor increases frontal-plane knee joint loading in stationary cycling. J Sport Health Sci 9, 258-264.10.1016/j.jshs.2019.07.011

Walter, J.P., D'Lima, D.D., Colwell Jr, C.W., Fregly, B.J., 2010. Decreased knee adduction moment does not guarantee decreased medial contact force during gait. Journal of Orthopaedic Research 28, 1348-1354

Wen, C., Cates, H.E., Zhang, S., 2019. Is knee biomechanics different in uphill walking on different slopes for older adults with total knee replacement? J Biomech 89, 40-47

Yocum, D., Weinhandl, J.T., Fairbrother, J.T., Zhang, S., 2018. Wide step width reduces knee abduction moment of obese adults during stair negotiation. J Biomech 75, 138-146.10.1016/j.jbiomech.2018.05.002

Figure Captions -

Figure 1. Average ensemble curves for A) Medial compartment contact force (MCF); B) Total knee joint contact force (TCF); C) Knee extensor muscle force; D) Knee flexor muscle force during one full crank cycle. * denotes significantly different first peak values for MCF and knee flexor muscle group between normal and wide QF. The shaded regions represent ± 1 SD.

Figure 2. Ensemble curves of the frontal-plane moment arm throughout the crank cycle at normal (dashed black line) and wide (solid black line). The vertical, dashed, gray line indicates the time of peak KAbM.

Figure 3. Mean EMG linear envelope curves for semitendinosus, biceps femoris, rectus femoris, vastus lateralis, vastus medialis, and gastrocnemius adapted from Ryan et al. (1992) (thin line), Savelberg (2003) (light gray line), as well as muscle activations from normal (dashed black line) and wide (thick black line) QF of the same muscles from this study estimated using static optimization while cycling 80 W and 80 RPM. The shaded regions represent ± 1 SD.

Figure 4. Ensemble curves for A) knee extension moment (KEM) and B) knee abduction moment (KAbM) during one full crank cycle. * denotes significantly different first peak values for KAbM between normal and wide QF. The shaded regions represent ± 1 SD.

Figure 5. Average curves for A) Medial compartment contact force (MCF) for the responder group; B) Total knee joint contact force (TCF) for the responder group; C) MCF for the non-responder group; D) TCF for the non-responder group.

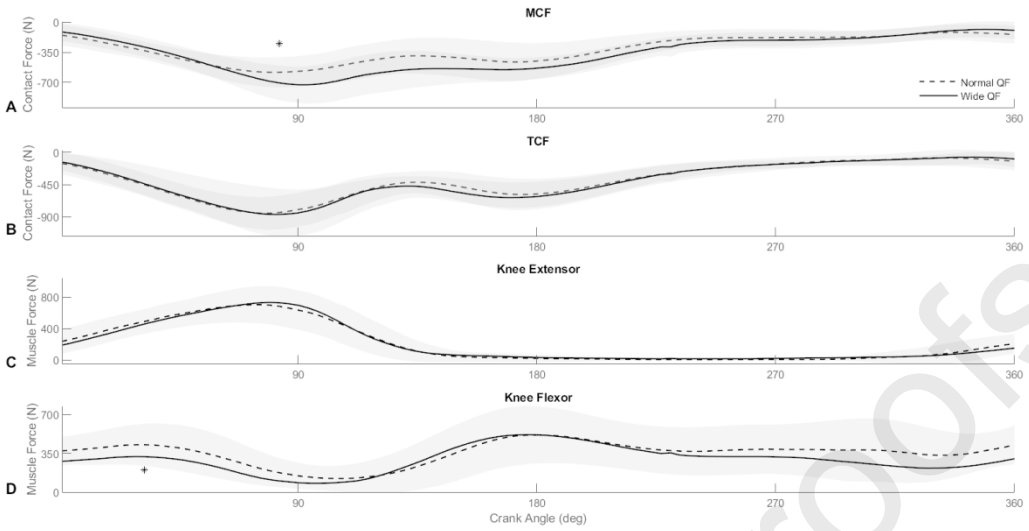

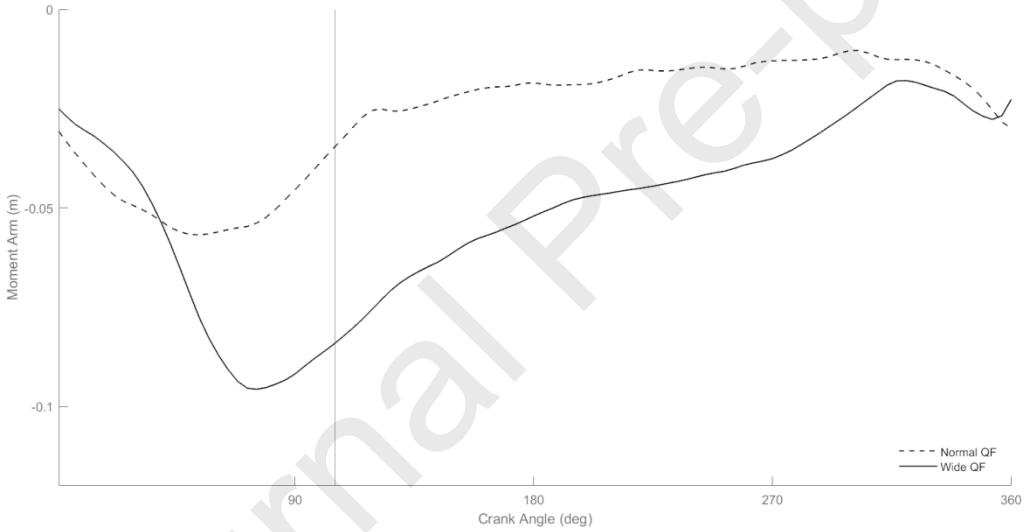

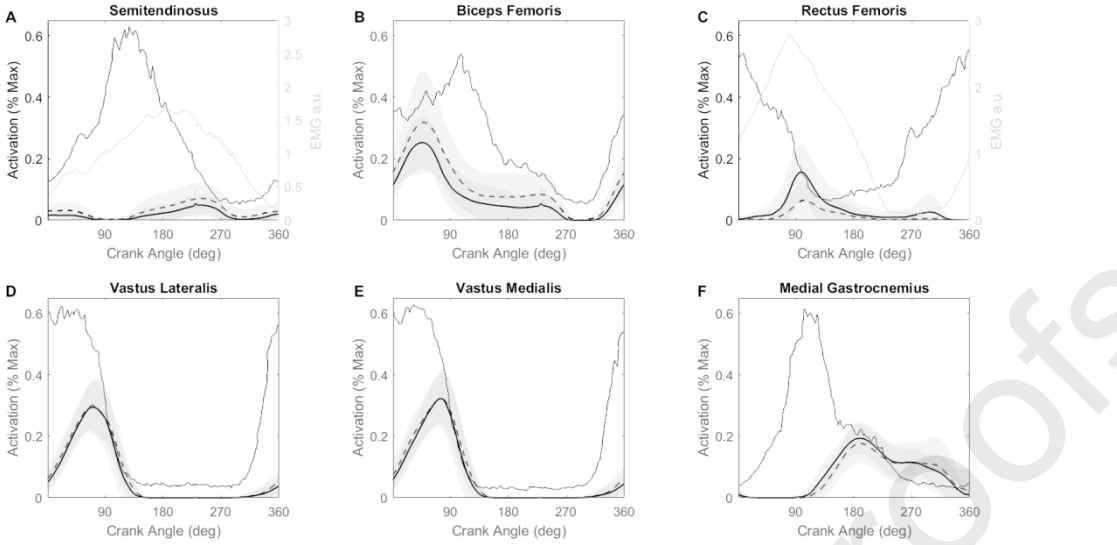

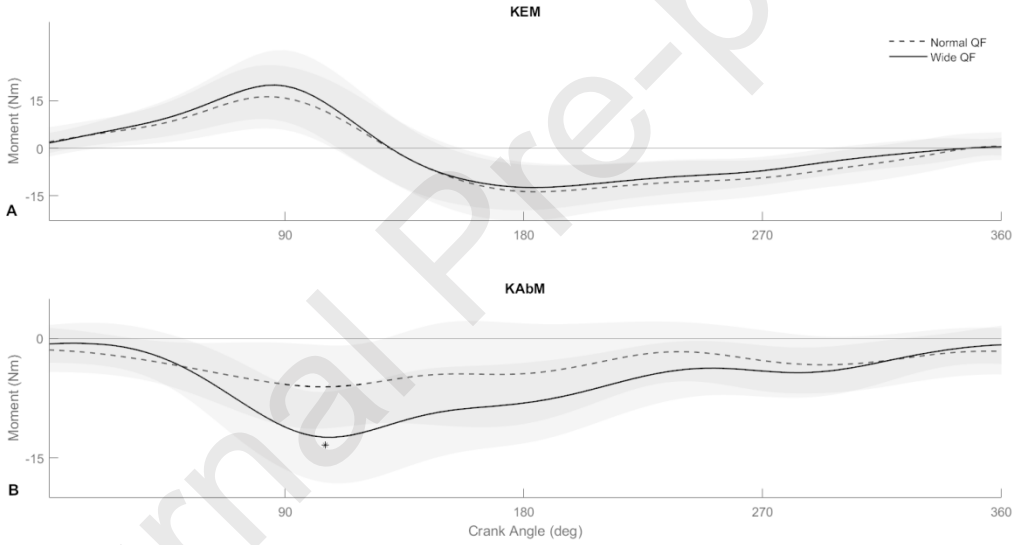

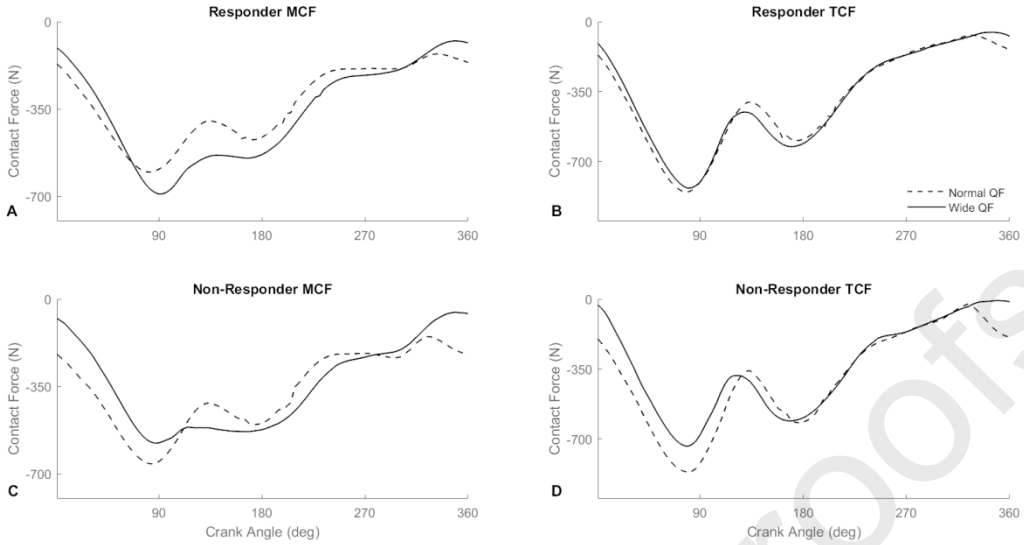

Table 1: Contact forces (N),joint moments (Nm), and frontal plane pedal reaction force (PRF) moment arm (m) at the time of peak KAbM with increased QF for the total sample, the subset group of the responders (n = 12), and the subset group of the non-responders (n = 4). Values presented are mean ± sd. **Bold** indicates statistical significance.

Variables	Normal QF	Wide QF	Cohen's d	p-value
		Total		
MCF	-639.1 ± 187.7	-727.2 ± 215.3	0.51	**0.025**
TCF	-882.9 ± 200.4	-894.8 ± 261.0	0.06	0.765
KAbM	-8.2 ± 5.6	-13.1 ± 5.8	0.87	**0.001**
KEM	18.2 ± 7.7	19.4 ± 10.1	0.16	0.511
		Responders		
MCF	-627.7 ± 164.0	-777.1 ± 216.8	0.91	**0.001**
TCF	-883.0 ± 215.0	-941.7 ± 287.0	0.27	0.130
KAbM	-7.8 ± 5.8	-13.3 ± 5.9	0.95	**0.001**
KEM	19.4 ± 8.3	21.2 ± 11.1	0.21	0.099
		Non-Responders		
MCF	-673.2 ± 223.2	-577.5 ± 140.2	0.43	
TCF	-882.9 ± 177.2	-754.3 ± 59.1	0.73	
KAbM	-9.6 ± 5.6	-12.6 ± 6.3	0.83	
KEM	14.9 ± 5.0	14.0 ± 2.7	0.18	
		Moment Arm		
PRF Moment Arm	0.062 ± 0.025	0.097 ± 0.015	0.39	**0.001**

Table 2: Peak power-phase muscle forces (N) with increased QF for the total sample, the subset group of the responders (n = 12), and the subset group of the non-responders (n = 4). Values presented are mean ± sd. **Bold** indicates statistical significance.

Variables	Normal QF	Wide QF	Cohen's d	p-value
		Total		
Knee Extensors	742.8 ± 196.2	754.3 ± 273.1	0.06	0.757
Knee Flexors	471.7 ± 209.0	378.4 ± 139.4	0.45	**0.046**
Rectus Femoris	101.3 ± 72.4	159.3 ± 96.4	0.80	**0.008**
Vastus Lateralis	346.9 ± 85.7	332.9 ± 97.0	0.16	0.032
Vastus Medialis	192.2 ±46.6	184.7 ± 52.6	0.16	0.033
Vastus Intermedius	182.4 ± 45.3	173.7 ± 51.1	0.2	0.251
Semitendinosus	23.6 ± 12.8	15.9 ± 8.8	0.59	**0.012**
Semimembranosus	219.9 ± 91.8	175.6 ± 89.1	0.37	0.066
Biceps Femoris Short Head	149.7 ± 50.9	185.4 ± 69.5	0.70	**0.002**
		Responders		
Knee Flexors	462.2 ± 180.0	361.7 ± 112.6	0.56	0.078
Knee Extensors	741.8 ± 217.7	794.3 ± 307.5	0.24	0.181
		Non-Responders		
Knee Flexors	499.99 ± 313.1	428.63 ± 214.7	0.23	
Knee Extensors	745.83 ± 136.8	634.3 ± 25.9	0.82	

Table 3: Linear Regression Equations for predicting MCF from corresponding KAbM, and KEM values at normal QF.

Regression Equation	c_1	c_2	c_3	R^2	RMSE
MCF = c_1 + c_2KAbM + c_3KEM	-272.768	24.337	-8.797	0.811	72.99
MCF = c_1 + c_2KAbM	-425.102	25.999	---	0.709	53.58
MCF = c_1 + c_2KEM	-495.765	-12.363	---	0.207	174.21

Note: Units of MCF (N), KAbM (Nm), KEM (Nm), RMSE (N).

Table 4: Linear Regression Equations for predicting MCF from corresponding KAbM, KEM, and QF.

Regression Equation	c_1	c_2	c_3	c_4	R^2	RMSE
MCF = c_1 + c_2KAbM + c_3KEM + c_4QF	-217.686	23.851	-11.927	34.416	0.874	69.08
MCF = c_1 + c_2KAbM + c_3QF	-419.287	26.706	42.077	---	0.627	96.46
MCF = c_1 + c_2KEM + c_3QF	-365.057	-14.52	-80.478	---	0.426	169.21
MCF = c_1 + c_2KAbM + c_3KEM	-211.566	22.685	-11.998	---	0.867	238.03
MCF = c_1 + c_2KAbM	-413.256	25.299	---	---	0.618	19.25
MCF = c_1 + c_2KEM	-402.296	-14.677	---	---	0.383	40.22

Note: Units of MCF (N), KAbM (Nm), KEM (Nm), QF (normal = 0, wide = 1), RMSE (N).